Effects of Chain-End Tethering on the Crystallization Kinetics of Poly(ε-caprolactone) Confined in an Identical Nanolamella

The effect of chain-end tethering to nanodomain interfaces on the crystallization kinetics of poly(ε-caprolactone) (PCL, $[(CH_2)_5\text{-CO-O-}]_n$) confined in an identical nanolamella has been investigated using synchrotron small-angle X-ray scattering (SR-SAXS) and differential scanning calorimetry (DSC). The PCL chains tethered at both chain-ends, one chain-end, and no chain-end were prepared from polystyrene-*block*-PCL-*block*-polystyrene copolymers with photo-cleavable groups at either or both of block junctions. The crystallinity of these PCL chains showed a sigmoidal time-evolution during isothermal crystallization, but the crystallizable temperature range was significantly different among them, indicating that the crystallization rate under identical crystallization temperatures depends greatly on the state of chain-end tethering.

Multi-component polymeric materials with nanometer-sized domains (nanodomains) have been attracting much attention because their properties can be flexibly controlled. Crystallization of constituent polymers drastically changes the physical properties of materials, so it is important to understand the crystallization mechanism of polymer chains spatially confined in various nanodomains. Such crystallization is known to yield unique morphologies as compared with that of bulk homopolymers without any confinement [1-3]. For example, the crystallinity of confined polymers is considerably reduced, the degree of which intimately depends on the nanodomain shape and size. It is also known that the crystallization of polymer chains confined in nanodomains is affected by chain-end tethering to nanodomain interfaces. We recently investigated the effect of chain-end tethering on the crystallization kinetics of poly(ε-caprolactone) (PCL) confined in various nanodomains using PCL-*block*-polystyrene (PCL-*b*-PS) diblock copolymers with photo-cleavable *o*-nitrobenzyl (ONB) groups between PCL and PS blocks [4-6]. It was found from these studies that the chain-end tethering controlled the crystallization mechanism of PCL chains as well as the crystallization rate and crystal orientation through a small change in their mobility. Here we further report on the effect of chain-end tethering on the crystallization kinetics of PCL chains confined in an identical lamellar nanodomain (nanolamella) [7].

We synthesized two kinds of lamella-forming PS-*b*-PCL-*b*-PS copolymers with ONB groups at either or both of block junctions. The PCL chains tethered at both chain-ends (T2-PCL, **a** and **a'** in **Fig. 1A**) confined in the nanolamella formed by microphase separation of the PS-*b*-PCL-*b*-PS copolymers were converted to those tethered at one chain-end (T1-PCL, **c**) or at no chain-end (T0-PCL, **b**) using the photo-cleavage reaction of ONB groups induced by UV irradiation. The vitrification of PS chains prevented macroscopic phase separation between PS and PCL homopolymers (or between PS homopolymers and PCL-*b*-PS copolymers) after

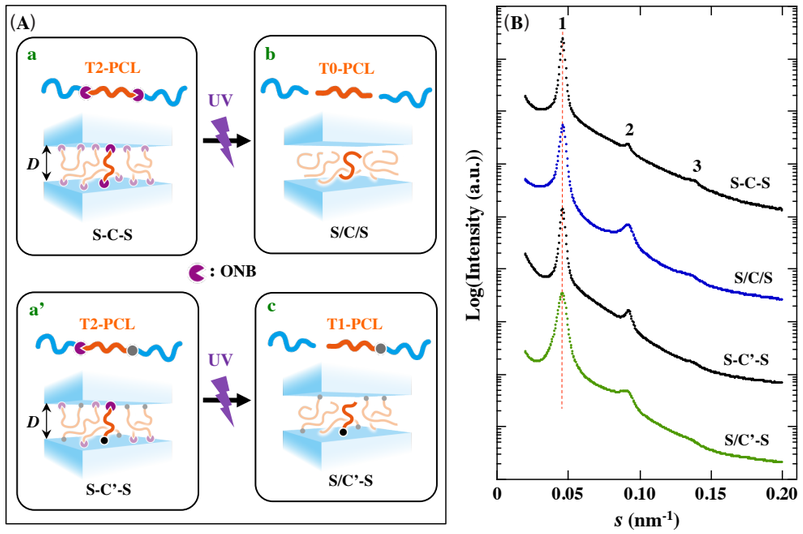

Figure 1: (A) Schematic illustration showing the sample preparation method used in this study. **(B)** SAXS curves of each sample. The PCL nanolamella thickness *D* is evaluated to be 11.0 nm for all samples.

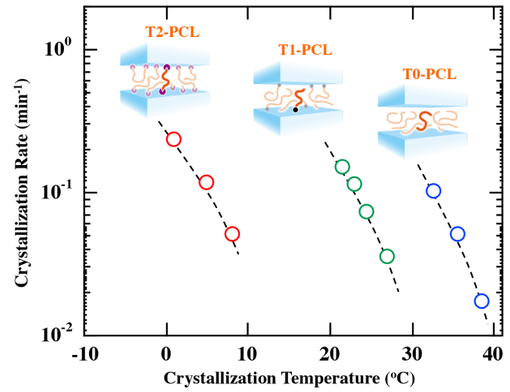

Figure 2: Crystallization rate (i.e., inverse of crystallization half-time) plotted against crystallization temperature for T2-PCL (red circles), T1-PCL (green), and T0-PCL (blue) all confined in an identical nanolamella with $D = 11.0$ nm.

photo-cleavage, and eventually we could prepare T0-PCL, T1-PCL, and T2-PCL all confined in an identical nanolamella. The formation of these nanolamellae was confirmed using SR-SAXS at BL-10C, and the heat of fusion of PCL chains (proportional to PCL crystallinity) was determined using DSC as a function of crystallization time to compare the crystallization kinetics among different samples.

Figure 1B shows the SAXS curves of various samples recorded after sufficient crystallization of PCL chains. They show several scattering peaks, the positions of which exactly correspond to a ratio of 1:2:3, indicating the formation of a lamellar microphase-separated structure, an alternating structure consisting of PCL and PS nanolamellae. The SAXS curves of amorphous samples also showed first- and second-order SAXS peaks at the same positions as the crystallized samples, suggesting that the lamellar microphase-separated structure formed in the amorphous state was completely preserved after crystallization, that is, the PCL chains crystallized within the existing nanolamella. The PCL nanolamella thickness *D* evaluated from the SAXS peak position was 11.0 nm for all the samples investigated. Therefore, it is possible to examine the crystallization kinetics of different PCL chains confined in an identical nanolamella.

The time evolution of PCL crystallinity during isothermal crystallization showed a sigmoidal change with a finite induction time for all samples, indicating that the crystallization of confined PCL chains was controlled by a conventional nucleation and growth mechanism usually observed in the crystallization of bulk homopolymers. That is, the chain-end tethering did not substantially affect the crystallization mechanism of confined PCL chains. However, the chain-end tethering significantly affected the crystallization rate during isothermal crystallization. **Figure 2** shows the crystallization rate (i.e., inverse of crystallization half-time) plotted against crystallization temperature T_c for T2-PCL, T1-PCL, and T0-PCL. It is clear that the T_c range is remarkably different among them. In particular, T2-PCL needs considerably lower T_c than T1-PCL and T0-PCL to crystallize in an experimentally accessible time scale, which arises from the largely decreasing mobility of T2-PCL due to both chain-ends tethering to nanolamella interfaces. Therefore, the crystallization rate is expected to be extremely different among T2-PCL, T1-PCL, and T0-PCL when compared under identical crystallization temperatures. This difference in crystallization rate can be qualitatively explained on the basis of energy barrier to form a critical nucleus in the secondary nucleation process.

REFERENCES

[1] R. M. Michell, I. Blaszczyk-Lezak, C. Mijangos and A. J. Müller, *Polymer* **54**, 4059 (2013).
[2] S. Huang and S. Jiang, *RSC Adv.* **4**, 24566 (2014).
[3] S. Nakagawa, H. Marubayashi and S. Nojima, *Eur. Polym. J.* **70**, 262 (2015).
[4] S. Nakagawa, K. Kadena, T. Ishizone, S. Nojima, T. Shimizu, K. Yamaguchi and S. Nakahama, *Macromolecules* **45**, 1892 (2012).
[5] S. Nakagawa, T. Tanaka, T. Ishizone, S. Nojima, Y. Kakiuchi, K. Yamaguchi and S. Nakahama, *Macromolecules* **46**, 2199 (2013).
[6] S. Nakagawa, T. Tanaka, T. Ishizone, S. Nojima, K. Kamimura, K. Yamaguchi and S. Nakahama, *Polymer* **55**, 4394 (2014).
[7] S. Nakagawa, T. Ishizone, S. Nojima, K. Kamimura, K. Yamaguchi and S. Nakahama, *Macromolecules* **48**, 7138 (2015).

BEAMLINE

BL-10C

S. Nojima[1], S. Nakagawa[2] and H. Marubayashi[1] ([1]Tokyo Inst. of Tech., [2]The Univ. of Tokyo)